ELSEVIER

Earth and Planetary Science Letters 181 (2000) 301–313

EPSL

www.elsevier.com/locate/epsl

On the role of microbes in the alteration of submarine basaltic glass: a TEM study

Jeffrey C. Alt [a,*], Pilar Mata [b]

[a] *Department of Geological Sciences, 2534 C.C. Little Building, The University of Michigan, Ann Arbor, MI 48109-1063 USA*
[b] *Departmento de Geologia, Facultad de Ciencias del Mar, Universidad de Cadiz, Campus Rio San Pedro, 11510 Puerto Real, Cadiz, Spain*

Received 2 February 2000; received in revised form 15 June 2000; accepted 21 June 2000

Abstract

The alteration of submarine basaltic glass that has been attributed to microbial activity was investigated via transmission electron microscopy in order to document glass alteration and to understand the chemical reactions that bacteria could utilize. The features that were examined occur within fresh glass at the alteration front and consist of 0.1–2.3 μm patches or tubes of phyllosilicates rimmed by 0.1–0.3 μm wide zones of altered glass. The altered glass has lost significant Mg, Fe, Ca and Na, slight amounts of Al and Mn, and exhibits an order of magnitude increase of K. This incongruent dissolution occurred at neutral to acid pH and temperatures $<90°C$. Phyllosilicates consist of montmorillonite–saponite with berthierine interlayers, plus a mica component. The phyllosilicates directly replace altered glass along the perimeters of the phyllosilicate areas, but the centers of many of these areas may be filled pore space formerly occupied by microbes that facilitated glass alteration. If so, the sizes of the bacteria ranged to less than 0.1 μm and into the range of nano-organisms. Iron in secondary products is essentially all ferrous, and is most likely mobilized from glass as the ferrous ion, possibly with the reduction of minor primary ferric iron in the glass. Small amounts of sulfide in secondary pyrite associated with altered glass may be derived from microbial reactions or from the glass itself. Net bulk chemical changes for altered glass plus phyllosilicates include losses of Si, Al, Fe, Mn, Ca and Na, plus possible slight losses of Ti. This material is redistributed into fracture-filling smectite along with significant K and Mg from seawater. The uptake of K requires the circulation of large amounts of seawater through fractures in the glass (>100 fracture volumes), which may be important for the supply of nutrients for microbial activity.

Keywords: bacteria; alteration; glasses; basaltic composition; halmyrolysis; TEM data

1. Introduction

Alteration features observed in basaltic glass of submarine pillow lavas have been attributed to microbial activity, leading to the inference that an extensive subsurface biosphere exists within the uppermost ocean crust [1–9]. It has been suggested that if microbes mediate the dissolution and alteration of basaltic glass, then this may play an important role in chemical exchange between seawater and the crust [2,7].

* Corresponding author. Fax: +1-734-763-4690; E-mail: jalt@umich.edu

0012-821X/00/$ – see front matter
PII: S0012-821X(00)00204-1

Alteration attributed to microbial activity in submarine basalt glass occurs in irregular patches that line cracks in the glass, with various evidence indicating the presence of microbes in these zones [1–9]. (1) The sizes and textures of many of these alteration features are similar to those produced by microbes in laboratory experiments with basaltic glass [1,2,7]. In the natural samples these comprise pits or spherules of varying sizes (0.3–10 μm) within fresh glass, as well as tubes or vermicular channels, 1–10 μm wide by up to 100 μm long, that extend into the glass. The tubes may be open or filled with secondary material. (2) The altered glass areas contain DNA and RNA specific to bacteria and archaea [3,4,6]. (3) The altered glass areas have elevated contents of C, N, P and K, which are attributed to the presence of microbial cells [4,6]. (4) Carbonate disseminated in altered glass rocks has $\delta^{13}C$ values that are lower than that of fresh basalt, consistent with the presence of oxidized organic carbon [6,9].

Volcanic glass can alter by different processes, depending on pH, temperature, solution composition and fluid/rock ratio [10–14]. Depending upon conditions, dissolution can be stoichiometric, or it may be incongruent with the formation of a hydrated and leached layer. The composition of altered basaltic glass associated with microbial activity appears highly variable and the associated secondary minerals are poorly documented [3–6]. A detailed study of glass alteration and rigorous identification of secondary minerals would help to determine the conditions of alteration and the chemical reactions associated with microbial activity in basalt glass, with a potential to identify what reactions microbes may utilize during glass alteration (e.g. Fe, Mn and/or S redox have been suggested [3,4,6]).

We have examined altered submarine basaltic glass using several techniques, including optical microscopy, scanning electron microscopy (SEM), transmission electron microscopy (TEM), analytical electron microscopy (AEM) and selected area electron diffraction (SAED) in order to document glass alteration and identify secondary products that have been attributed to microbial activity. Our objectives are to understand the chemistry and processes of glass alteration and how these relate to microbial activity in the ocean crust.

2. Sampling and methods

We examined several samples of glassy basalt pillow rims by optical microscopy and SEM from ODP Holes 504B and 896A, located in 6 Ma crust of the eastern Pacific [15] and selected one for detailed analyses (Sample 504B 21R4, 101–102, No. 1250, from 152 m subbasement). Microbial effects in altered glass have previously been described in great detail from these sites [3,4,6,8], and Furnes et al. [9] provide data for a piece of glass adjacent to our sample 1250. Furnes and Staudigel [8] suggest that ~75% of the glass alteration in this shallow region of the crust is microbial in origin.

Polished thin sections were made for preliminary observations by optical microscopy. SEM observations using back-scattered electron (BSE) imaging were performed on both polished thin sections and ion-milled specimens using an Hitachi S-3200N SEM, equipped with a Noran X-ray energy-dispersive system (EDS), and operated at 20 kV. Following optical and BSE examination, selected areas were removed from sticky wax thin sections, ion-milled and carbon-coated. Ion-milled samples were then re-examined by optical microscopy and SEM–BSE in order to map out alteration textures and directly relate subsequent TEM data to the other scales of observation. TEM observations and AEM analyses were obtained with a Philips CM12 scanning-transmission electron microscope, operated at an accelerating voltage of 120 kV and a beam current of ~10 μA. Lattice fringe images of phyllosilicates were obtained using 001 reflections. The initial focus was controlled manually by minimizing contrast, and images were taken at over-focus conditions (1000 Å) [16].

X-ray EDS spectra were obtained using a Kevex Quantum detector. A raster (2000×2000 Å maximum size) in scanning mode was used to minimize alkali diffusion and volatilization. Quantitative AEM chemical analyses were calculated from spectra using ion-milled standards of

Table 1
Representative AEM analyses of fresh and altered glass and phyllosilicates

Wt% oxide	Glass			Altered glass			Phyllosilicates			
	EMPA[a]	AEM[b]	1σ	bO703-9	bO759-1	bO759-P	sO657-5	sO721	sO727	sO732
SiO_2	50.43	50.13	2.73	56.68	70.79	65.76	41.22	56.33	58.30	46.59
Al_2O_3	15.15	15.74	0.47	19.18	13.93	16.49	16.16	15.18	14.15	16.88
MgO	8.67	7.04	0.90	3.82	0.99	1.50	12.68	8.32	8.83	13.26
FeO	9.45	9.39	0.63	4.21	1.27	2.65	16.53	7.53	8.93	12.63
TiO_2	1.05	0.76	0.09	0.77	1.20	1.07	0.71	1.25	1.64	0.85
MnO	0.14	0.29	0.19	0.00	0.00	0.00	1.10	0.57	0.00	0.94
CaO	12.98	13.38	0.82	6.44	1.97	2.61	1.37	1.48	0.80	1.09
Na_2O	2.14	2.74	0.32	2.65	2.52	1.34	1.57	2.80	1.25	2.20
K_2O	0.03	0.12	0.17	1.24	2.33	3.58	3.67	1.55	1.09	0.55
Formulas										
Si							6.00	7.47	7.66	6.44
Al(IV)							2.00	0.53	0.34	1.56
Al(VI)							0.78	1.85	1.85	1.19
Mg							2.75	1.65	1.73	2.73
Fe							2.01	0.83	0.98	1.46
Ti							0.08	0.13	0.16	0.09
Mn							0.14	0.06	0.00	0.11
VI Total							5.76	4.52	4.72	5.58
Ca							0.21	0.21	0.11	0.16
Na							0.44	0.72	0.32	0.59
K							0.68	0.26	0.18	0.10
Interlayer							1.33	1.19	0.61	0.85

AEM analysis of fresh glass normalized to 100%, altered glass and phyllosilicates normalized to 95% (see text). Formulas based on 22 oxygens, all Fe as Fe^{2+}.
[a]EMPA from M. Fisk (personal communication).
[b]Average of five AEM analyses.

paragonite, muscovite, albite, clinochlore, fayalite, rhodonite and titanite to derive k-ratios, following the procedure of Jiang et al. [17]. Peacor [18] presents a detailed discussion of AEM analytical techniques and errors, showing that AEM and electron microprobe analyses (EMPA) should give comparable results. The AEM analyses in Table 1, however, have somewhat larger errors than EMPA, which are typically within 2% for major and 5% for minor elements. At the very low K_2O content of fresh glass, the AEM analysis is high relative to that of EMPA, but at the higher K_2O concentrations characteristic of the altered glass and phyllosilicates the accuracy of the AEM analyses should be much greater and comparable to EMPA analyses (Table 1) [18]. The MgO content of glass by AEM is slightly low compared to EMPA, which could slightly affect mineral formulas, but this does not affect relative chemical changes determined by the comparison of AEM analyses of fresh and altered glass.

3. Results

3.1. Textures

Glass alteration textures in all the samples we examined are typical of those previously described and attributed to microbial alteration of glass [1–3,5,6]. Large areas of glass are pristine and optically isotropic, but fractures in the glass are lined with irregular altered zones (Fig. 1). Irregular or vermicular tubes and channels, 1–5 μm wide, extend up to tens of μm into the adjacent unaltered glass and are filled with secondary material. Also present are 0.3–2.5 μm spots concentrated in the unaltered glass near the alteration front. These

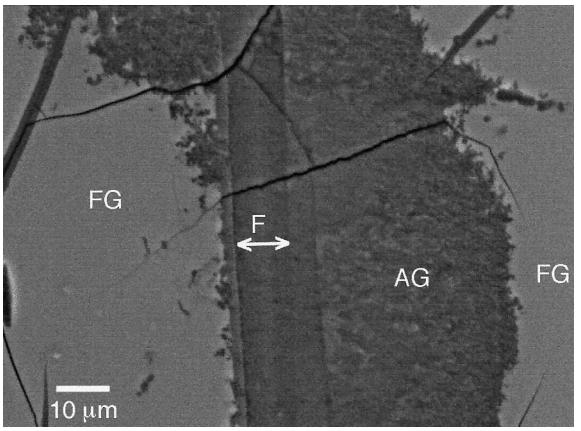

Fig. 1. BSE image of typical glass alteration textures. Fresh glass (FG), altered glass (AG) and formerly open fracture (F) filled with secondary smectite are indicated. The contact between fresh and altered glass is characteristically irregular, with small spherulitic and vermicular bodies extending into the fresh glass. The asymmetric development of altered glass around the fracture is typical of microbial effects [8]. This altered glass material is identical to that in other samples from Hole 504B and from nearby Hole 896A that contain DNA and RNA and high contents of P, N and C [4,6,9].

features are circular to elliptical and irregular in cross-section. Furnes et al. [3] referred to these spots as spherical bodies, but three dimensionally they may be filled or solid tubular features, and there appears to be a continuum from the tiny spots to the larger tubes and channels. Fracture fillings can be identified by their sharp, parallel outlines and fibrous, crystalline nature in transmitted light and in BSE images. Secondary pyrite is common in small amounts as <1–5 μm cubes and irregular grains scattered throughout altered glass areas and in smectite veins. Secondary pyrite contains trace amounts of Ni, but is clearly distinct texturally and compositionally from igneous sulfides, which have a globular morphology and contain significant Cu and Ni. Trace iron oxyhydroxide is present along a fracture associated with secondary pyrite in sample 1250, and may be a late oxidation product of pyrite. Other phases in this sample include saponite replacing olivine, and trace phillipsite filling the center of a saponite-lined fracture. Secondary phases in other basalts in the upper 300 m of basement include

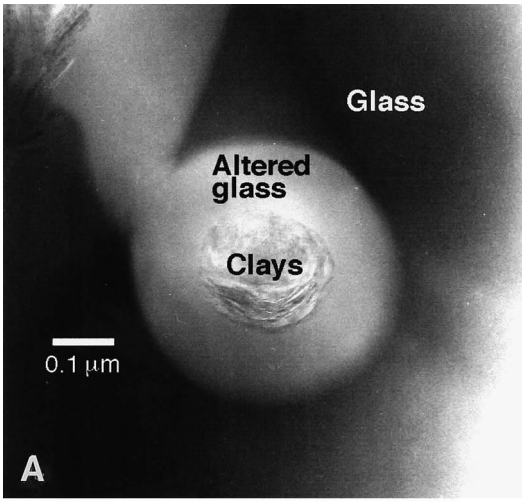

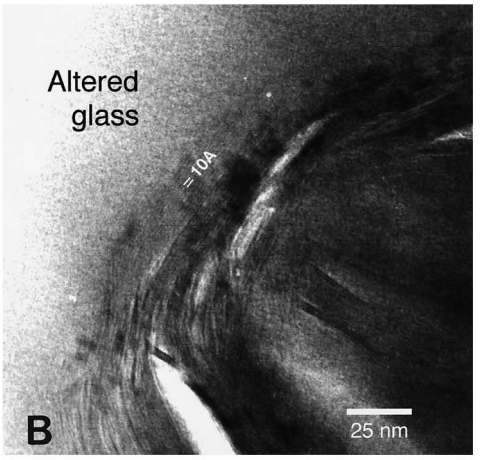

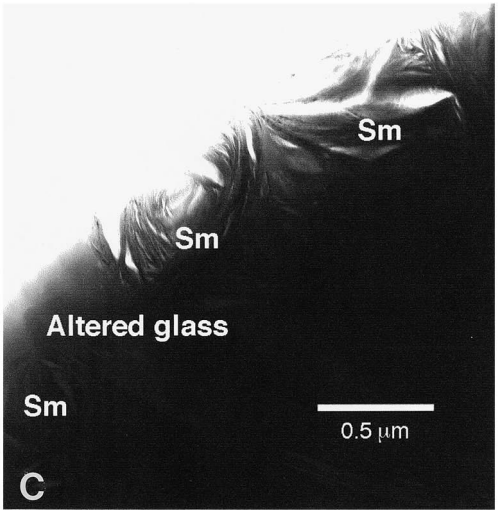

Fig. 2. TEM images of altered glass. (A) 0.3–2.5 μm altered 'spots' in fresh glass (at the alteration front in Fig. 1) consist of a 0.1–0.3 μm rim of altered glass surrounding a phyllosilicate core. (B) High resolution TEM image showing lattice fringes of partially collapsed smectite. The concentrically arranged phyllosilicate packets formed by direct replacement of glass give way to a different texture at the centers of the spots (right side of B and upper center of A), which may result from the filling of open pores formerly occupied by microbes. (C) The tiny altered spots coalesce to form zones of 'altered glass' along fractures (altered glass in Fig. 1), with this altered material consisting of 0.1–2.0 μm ellipsoidal aggregates of phyllosilicate (Sm) in a matrix of altered glass as shown here.
←

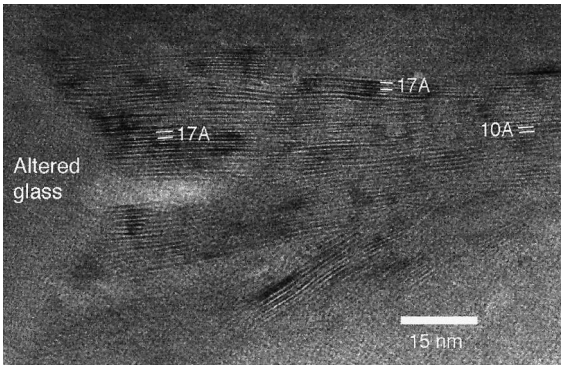

Fig. 3. High-resolution TEM image of secondary phyllosilicates replacing altered glass along a fracture. Lattice fringe image illustrating 10 Å smectite layers resulting from the dehydration and collapse of 14 Å smectite layers. Note the presence of 7 Å layers, in some cases forming regular 17 Å interstratification with 10 Å smectite.

smectite, celadonite, aragonite, calcite, phillipsite, iron oxyhydroxides and minor pyrite [15].

Three types of material have been recognized through a combination of TEM imaging, SAED patterns and AEM analyses: fresh and altered glass and phyllosilicates. Fresh glass has uniform contrast and composition, and exhibits no electron diffraction pattern, consistent with amorphous material. Altered glass is also amorphous and displays no diffraction pattern, but it differs significantly in contrast and composition from fresh glass and is easily damaged under the electron beam.

With TEM we examined 31 of the alteration features set in unaltered glass. These consist of a 0.1–0.3 μm wide rim of altered glass surrounding a core of secondary phyllosilicates (Fig. 2A). Along the margins of the phyllosilicate areas, the phyllosilicates display generally curved and concentric layers that reflect the overall circular to elliptical structure. High resolution TEM imaging of a subset of these features show a continuous transition between the surrounding altered glass and the crystalline phyllosilicates (Fig. 2B). Individual phyllosilicate layers can be traced along their length to end in altered glass and the layer silicates grade outward into the enclosing altered glass. These textures indicate that the phyllosilicates formed by direct replacement of altered glass. The central portions of these phyllosilicate areas, however, commonly have different textures. Such changes in contrast in TEM images can be the result of different orientations of smectite crystals, which may reflect precipitation from solution into open pores (Fig. 2A,B). If these latter textures represent formerly open pores, their sizes ranged from 0.04 to about 2 μm.

Closer to the former open fracture the alteration features are more abundant and coalesce, with phyllosilicate aggregates set in a matrix of variably altered glass (Fig. 2C). Much of what appears by optical microscopy or SEM to be altered glass or phyllosilicate replacement of glass (altered glass in Fig. 1) consists of this mixture of altered glass and phyllosilicates. Within this zone, altered glass between the phyllosilicate aggregates is also directly replaced by phyllosilicates (Fig. 3).

3.2. altered glass composition

Representative AEM chemical analyses of fresh and altered glass and secondary phyllosilicates are presented in Table 1, and are plotted with additional analyses in Fig. 4. The altered glass exhibits depletions of Mg, Fe, Mn, Ca and Na, and enrichment of Si, Al, Ti and K compared to fresh glass. The cation losses are real, but there is no source of Si, Al or Ti external to the glass and these elements may be passively enriched as material is lost and the density of the altered glass decreases [19–22]. AEM analyses are based on peak intensity ratios and elements are normalized to a constant number of cations or oxygen atoms

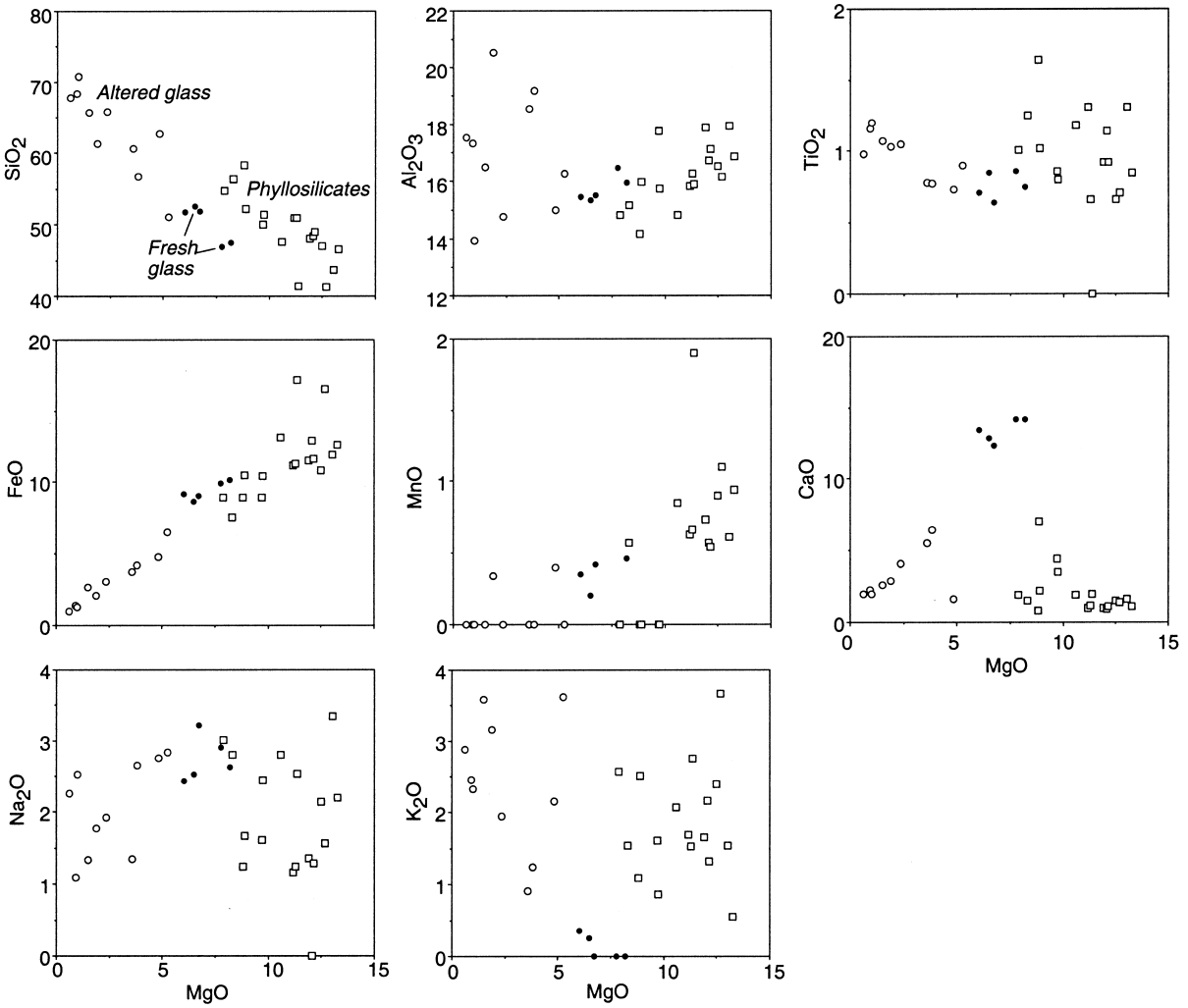

Fig. 4. AEM chemical analyses of fresh and altered glass and secondary phyllosilicates, plotted as oxide weight percent versus weight percent MgO. Analyses of fresh glass normalized to 100%, altered glass and phyllosilicates to 95%. Normalization of altered glass does not take into account density decrease and loss of material (see text).

and to an arbitrary total oxide weight percentage [16,18]. The effects of density decreases and corresponding low oxide totals are therefore not apparent in Table 1 or Fig. 4.

One way to approach this problem is to examine the mass balance. Clearly, much of the material comprising the phyllosilicates in the alteration patches is derived from the glass that was dissolved or replaced plus the altered glass rim. Mass balance calculations were made assuming that the alteration features are cross-sections of cylinders that are altered to a constant thickness (0.1 μm) rim of altered glass plus a phyllosilicate core. The mean compositions for fresh and altered glass and phyllosilicate were used, with densities of 2.9 and 2.5 for fresh glass and phyllosilicates, respectively. If Al is assumed immobile during the conversion from fresh to altered glass, this requires a net gain of Ti by the combined altered glass rim plus phyllosilicate core, which is clearly unreasonable. If Ti is assumed immobile during the transition from fresh to altered glass, then the

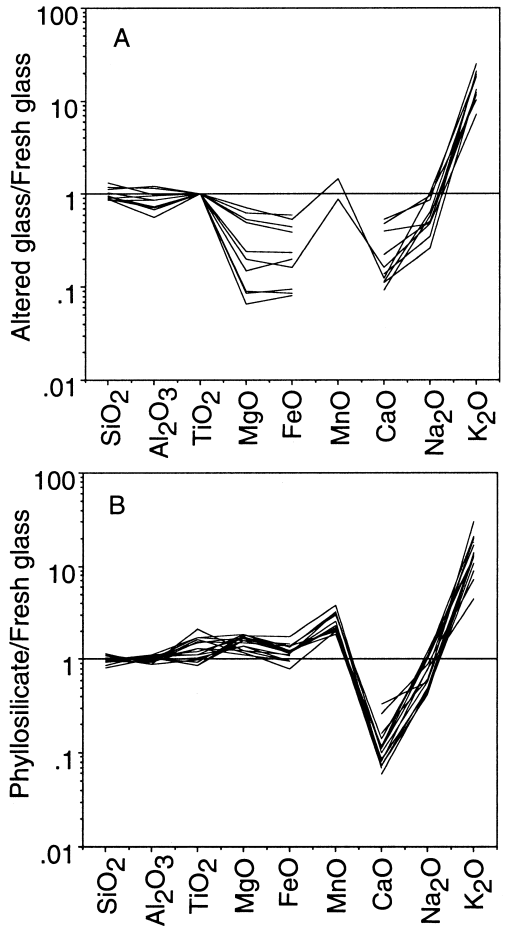

Fig. 5. Spidergrams illustrating compositions of altered glass and phyllosilicates compared to unaltered glass. Altered glass is normalized to constant TiO_2 with respect to fresh glass, and all data are normalized to mean fresh glass composition by AEM from Table 1. Data points are not plotted where no oxide was detected in AEM analysis (e.g. several MnO analyses of altered glass).

conversion of fresh to altered glass plus phyllosilicate results in net losses of Si, Al, Fe, Mn, Ca and Na, plus slight losses of Ti at small cylinder diameters. K_2O contents consistently increase by a factor of 12. It makes little or no difference to these results if the features are assumed to be spheres, or if Si is assumed immobile (Si and Ti behave similarly and the concentrations of both increase by $\sim$20% in the altered glass relative to fresh glass). The density of the altered glass decreases, to a value of 2.3 g cm^{-3} if Si and Ti are immobile.

Fig. 5A shows that for constant Ti the fresh to altered glass transition results in losses of Al, Mg, Fe, Ca and Na, and a significant gain of K. Relative to fresh glass, phyllosilicates also exhibit losses of Ca and Na, but can account for the Mg and some of the Fe lost from the altered glass (Fig. 5B). Fracture-filling smectites are also sinks for other elements lost during the alteration of glass (Fe, Mn, Ca, Na), as well as Mg and K from seawater. The strong K enrichment of the altered glass rims (up to 3.6 wt% K_2O, Table 1) must be derived from seawater.

3.3. Phyllosilicate mineralogy

TEM and AEM analyses indicate that the phyllosilicates are composed of several components, including smectite, berthierine and mica. Lattice fringe images show that most layers are smectite, having spacings that vary from 10 to 12 Å depending on the degree of dehydration and layer collapse caused by the instrument vacuum and interaction with the electron beam (Fig. 3). The layers comprise packets up to 17 layers thick, but more commonly form packets 4–5 layers thick intercalated with elongate voids as a consequence of collapse in the TEM (Figs. 2B and 3). The crystals of smectite occur as imperfect and anastomosing layers with numerous edge dislocation-like layer terminations. Although much of the phyllosilicate material consists of smectite-like layers, 7 Å layers are also present and commonly form regular interstratifications with the 10 Å layers resulting in 17 Å spacings (Fig. 3). This interlayered material forms sequences up to four units thick (ca. 70 Å) and exhibits layer terminations and low angle contacts with packets of smectite. Besides smectite and the 7 Å phase, tentatively identified as berthierine, the presence of a mica component within the phyllosilicates is suggested from AEM analyses (see below).

The phyllosilicates in the glass alteration features exhibit a range of compositions, but compared to fresh glass they are significantly enriched in Mg, Fe, Mn and K, and depleted in Ca and Na (Table 1 and Figs. 4 and 5). The phyllosilicates

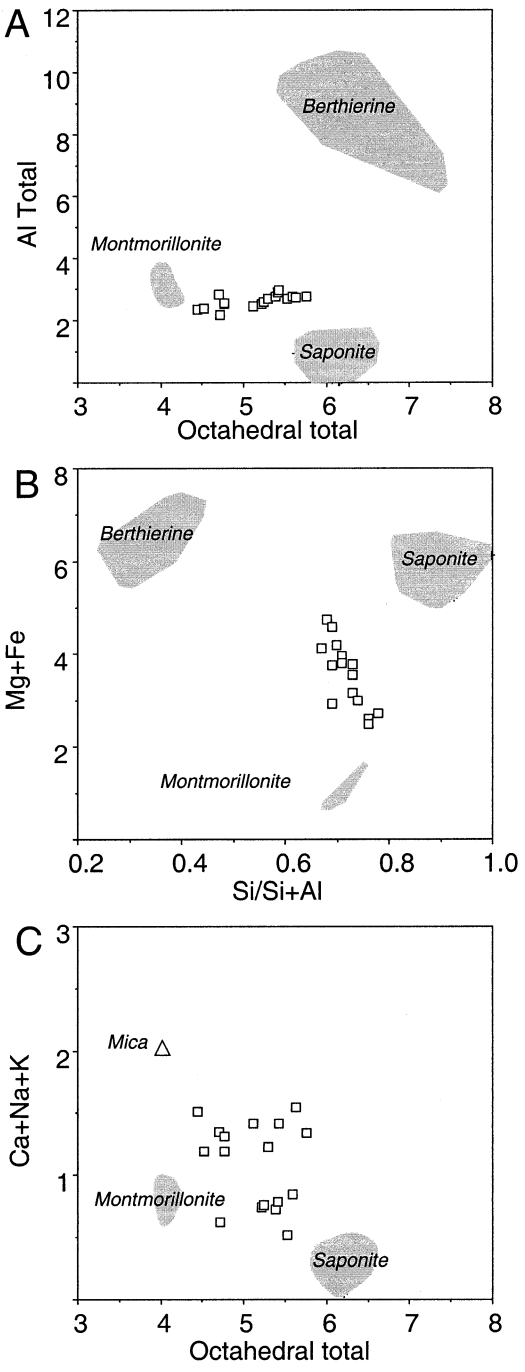

Fig. 6. AEM analyses of phyllosilicates calculated as smectite formulas on the basis of 22 oxygens, with all iron as ferrous. Phyllosilicates associated with altered glass fall on a trend from montmorillonite to a composition intermediate between saponite and berthierine (A and B). Higher interlayer cation contents (C) suggest the presence of a mica component. Data for saponites from Hole 504B [15] and berthierine [38] calculated in the same manner. Fields for montmorillonite and dioctahedral mica from Newman and Brown [38], with all iron as ferric.
←

are roughly similar in composition to saponite, the most typical low-temperature alteration product of submarine basalts [23]. The phyllosilicates in the glass, however, contain greater amounts of Al, have lower Fe+Mg and Si contents, and have lower octahedral cation totals than saponite (Fig. 5A,B). The relatively high Al contents reflect the primary substrate: the Al_2O_3/SiO_2 ratio of smectite replacing glass in submarine basalts is identical to that of the glass it replaces [24], having higher values in basaltic glass at pillow rims ($\sim$0.25–0.33) and lower values for silicic interstitial glass in pillow interiors (0.11–0.20). The phyllosilicates filling the centers of fractures also differ slightly in composition from those replacing glass: the former contain less Al and greater amounts of Mg than the latter, making the center of the fracture fillings more similar compositionally to typical saponite.

The phyllosilicates associated with altered glass plot in an array stretching from a composition near montmorillonite to one intermediate between those of saponite and berthierine, consistent with intergrowths and interlayering of these phases (Fig. 6A,B). Limited solid solution between dioctahedral (Al-rich) and trioctahedral (Mg-rich) smectites implies that the intermediate compositions in Fig. 6A represent mixtures or perhaps interlayering of di- and trioctahedral smectites [25]. High interlayer cation contents of many of the analyses, however, suggest that a mica component is also present (Fig. 6C).

4. Discussion

Basaltic glass can alter by different processes, depending on solution composition, temperature and fluid/rock ratio [10–14,22]. Dissolution is stoichiometric in laboratory dissolution experiments under alkaline conditions, whereas at neutral to

acid conditions network-modifier cations (Mg, Fe, Ca, Na) exhibit incongruent behavior with respect to silica and are leached in exchange for protonation and hydration of the glass surface. A thin (up to a few μm) leached layer resulting from incongruent dissolution of basalt glass has been observed or inferred in experiments [10–12], but has only rarely been observed at the fresh glass alteration front in natural samples [26]. Although high resolution observations are scarce, natural basalt glasses typically exhibit a sharp transition from unaltered glass to alteration products [19–21,27–29], perhaps reflecting the low water/rock mass ratios in natural systems compared to experiments [30]. The alteration products are mainly saponitic smectite and 'palagonite,' which is the partly recrystallized residual leached layer that results from passage of the reaction front through the glass. This material is composed of amorphous material and poorly crystalline smectite resulting from further alteration but zeolites, carbonates and oxides may also be present [19,26]. Submarine alteration of basaltic glass at pillow rims results in losses of essentially all major and minor cations except Ti and Fe, which can be passively accumulated, and K, which exhibits significant uptake [19–21]. If secondary minerals filling fractures in the glass are taken into account, however, many of the losses from the glass can be accounted for or even reversed (e.g. uptake of Mg into smectite, Na in zeolites, etc.) [19,20].

Convincing evidence exists for the local involvement of microbes in submarine alteration of basaltic glass, i.e. where long open tubes extend into fresh glass and where DNA, carbon or cell-like objects have been identified within such channels [3–5]. The interpretation here is that microbes mediate the dissolution of the glass, effectively tunneling into fresh glass. DNA and enrichments of carbon and phosphorus also occur within altered material behind the alteration front, as in the altered glass zone in Fig. 1 [3,6,9], indicating the presence of micro-organisms in these zones as well. When this study began, the working hypothesis was that the 0.1–2.5 μm alteration spots were formerly open holes that were initially formed and occupied by bacteria, then later filled with phyllosilicates. Our results, however, indicate that much of the area of these alteration spots consists of altered glass plus phyllosilicates formed via direct replacement of altered glass. Thus, any open pores or tubes that could have been occupied by bacteria were significantly smaller than the overall size of the alteration spots, smaller even than the patches of phyllosilicates within the spots. The areas that could have been former pore spaces range in size from 0.04 to about 2 μm. The larger end of this size range is typical of bacteria, but the smaller sizes fall in the realm of nano-organisms [31]. Thus a wide range of sizes of bacteria may exist in glassy basalt samples, perhaps representing different types of organisms.

Temperatures of alteration at the level in the crust where sample 1250 resided ranged from near 0 up to 90°C, and the current temperature at this depth is about 70°C [15]. The presence of the silica-rich altered glass in sample 1250 indicates incongruent dissolution at neutral to acid pH conditions [12,14]. Low pH can be maintained inorganically by the precipitation of clay minerals during seawater interaction with basalt glass: the combination of silica released from glass with seawater Mg^{2+} and $(OH)^{-}$ to form phyllosilicates results in the acid conditions that are typically observed in laboratory experiments over a broad range of temperatures (70–400°C [32]. Bacteria can additionally influence the microenvironment at the fresh/altered glass reaction front. Organic acids and ligands produced by bacteria can increase glass dissolution rates and change the stoichiometry of glass dissolution by affecting surface reactions and the complexation of ions in solution [33–35].

The observation of open $\sim$1 μm diameter tubes extending tens of microns into fresh volcanic glass in many samples and of similar features filled with phyllosilicates in other samples [1–6] suggests a two-stage process, with the initial formation of open tubes by microbially enhanced dissolution of glass followed by precipitation of phyllosilicates within the open space. TEM observations, however, suggest additional processes: the partial dissolution of glass surrounding the tubes, probably during the formation of the open tube, and replacement of the walls of the tubes by phyllosilicates. The latter may have oc-

curred during occupation of the pore by bacteria, but probably before filling of the pore with phyllosilicates. Microbes and associated biofilms in natural and experimental systems can accumulate elements such as Fe, Si and Al (as well as P) [2], and such material has been suggested to be the precursor for phyllosilicate formation in some environments [36]. Microbes thus may be involved in biomineralization in submarine basaltic glass, but we have no direct evidence for a microbial role in the formation of phyllosilicates in the features that we investigated.

Elevated K_2O contents of 1–2 wt% for altered material compared to fresh glass (0.3%) have been interpreted to be the result of accumulation in microbial cells [3]. Torsvik et al. [6] suggest that because K is lost from dead cells, the high K contents require the presence of living cells. Our TEM/AEM results indicate chemical variations on the scale of $\sim$0.1 μm, and that altered glass can contain large amounts of K_2O (up to 3.6 wt%). Thus, previous EMPA of such material must include varying combinations of altered glass and secondary phyllosilicates, and live cell material is not required to account for the high K_2O contents. Altered glass and phyllosilicates contain on average about 2 wt% K_2O, which was taken up from seawater. Assuming quantitative extraction of K from seawater, this requires a minimum integrated seawater/rock mass ratio of $\sim$43. If the volume of altered glass along a fracture is roughly the same as that of the formerly open fracture (e.g. Fig. 1), then at least 130 volumes of seawater have flowed through each fracture. This suggests that if microbial activity is involved, the circulation of significant amounts of seawater-derived fluids may be required to provide essential nutrients. This is consistent with more abundant microbial effects in the uppermost 200–300 m of the oceanic basement, where porosity, permeability and seawater circulation are greatest [8].

Losses of Fe and Mn from altered glass have been suggested to reflect utilization by microbes, either through oxidation or as electron acceptors under anaerobic conditions [3,4,6]. The iron and manganese contents of the secondary phyllosilicates are somewhat variable, but we find no evidence for discrete Fe- or Mn-oxide phases. Celadonite is another oxidized secondary phase that occurs in the upper few hundred meters of oceanic basement, coinciding with the zone of most abundant microbial effects in glass [8], but sample 1250 does not contain this mineral. In contrast, our data indicate a reducing environment, with iron incorporated into the secondary phase as ferrous ion. The compositions of phyllosilicates associated with altered glass are accounted for by partitioning the total iron present as ferrous iron into berthierine and saponite [37,38]. This suggests the mobilization of iron from glass as the ferrous ion, possibly with the small amount of ferric iron in the glass (about 10% of the total Fe [39]) being reduced.

The common presence of pyrite associated with altered glass and smectite veins is consistent with the inference of reducing conditions, although the source of sulfur remains uncertain. The low Ni contents and absence of Cu in secondary sulfides are distinct from recrystallized immiscible igneous sulfide globules, but secondary pyrite could have formed from primary igneous sulfide that was dissolved in the silicate glass (about 900 ppm S [40]). Alternatively, microbes could utilize sulfur redox reactions during the dissolution of basalt glass [6], and the sulfide may be derived from microbial reduction of seawater sulfate. The $\delta^{34}S$ values of altered pillow basalts from the ocean crust are typically about 0 to -35‰ [40,41], within the range for microbial pyrite in sediments. These low values for basalts have also been explained by inorganic reactions, however [40,41]. Very high sulfide contents (1 wt%) and low $\delta^{34}S$ values (to -43‰) occur in some oceanic serpentinites as the result of microbial sulfate reduction, with microbial communities supported by the hydrogen and methane produced during serpentinization [42]. Perhaps similar reactions could occur at the glass surface or in mafic minerals (olivine) in the glass.

Where the alteration spots coalesce in 'altered glass' zones closer to the formerly open fracture, between phyllosilicate spherules there are areas of altered glass that are also directly replaced by phyllosilicates (Fig. 3). Thus, alteration continues after formation of the patches and their coalesc-

ing into the 'altered glass' zones. This remaining altered glass may ultimately be transformed further into phyllosilicates or other minerals (zeolites, carbonates). Direct replacement of altered glass by phyllosilicates suggests that microbes are not involved in this reaction, however.

5. Summary and conclusions

Alteration features in submarine volcanic glass investigated via TEM comprise 0.3–2.5 μm areas in cross-section, having phyllosilicate cores and 0.1–0.3 μm wide rims of altered glass. The altered glass exhibits decreased density, significant losses of Mg, Fe, Ca and Na, slight losses of Al and Mn, and an order of magnitude gain of K. Si and Ti remain constant or increase slightly by passive accumulation. This incongruent dissolution of glass occurs at neutral to acid pH conditions at temperatures $<90°C$, and was probably enhanced by the presence of bacteria.

Phyllosilicates consist of montmorillonite–saponite with berthierine layers, plus a mica component. The phyllosilicates at the periphery of the phyllosilicate areas form by direct replacement of altered glass, but the cores of these patches may be former pore spaces formed by bacterial dissolution of glass. The sizes of these potential former pores suggest that bacteria ranged to as small as ~ 0.04 μm in size. As alteration proceeds further, the isolated alteration features coalesce into areas of phyllosilicate set in a matrix of variably altered glass, and phyllosilicates locally replace the altered glass between phyllosilicate aggregates. This latter replacement is probably not directly influenced by microbial activity.

There is no evidence for discrete Fe or Mn oxides that could result from microbial processes. Iron is mobilized from glass as ferrous iron, possibly with the reduction of the small amount of ferric iron in the glass. Small amounts of secondary pyrite are associated with altered glass, with the sulfide derived either from microbial reactions or from the glass itself.

Net bulk chemical changes for altered glass plus phyllosilicates include losses of Si, Al, Fe, Mn, Ca and Na, plus possibly slight losses of Ti. This material is redistributed into fracture-filling smectite, along with K and Mg from seawater. Uptake of K requires the circulation of significant volumes of seawater-derived fluids through fractures in the glass, which may be an important control on the occurrence of microbial activity in oceanic basement.

Acknowledgements

This work was supported in part by NSF OCE-9633353 and OCE-9818887. The authors thank Carl Henderson for technical assistance, and Jean-Louis Crovisier, Jose Honnorez, Donald Peacor and Peter Schiffman for discussions and comments. This paper benefitted significantly from helpful reviews by Martin Fisk, Harald Furnes and Hubert Staudigel.*[FA]*

References

[1] I. Thorseth, H. Furnes, M. Heldal, The importance of microbiological activity in the alteration of natural basaltic glass, Geochim. Cosmochim. Acta 56 (1992) 845–850.
[2] I. Thorseth, H. Furnes, O. Tumyr, Textural and chemical effects of bacterial activity on basaltic glass: an experimental approach, Chem. Geol. 119 (1995) 139–160.
[3] H. Furnes, I.H. Thorseth, O. Tumyr, T. Torsvik, M.R. Fisk, Microbial activity in the alteration of glass from pillow lavas from Hole 896A, Proc. ODP Sci. Results 148 (1996) 191–206.
[4] S.J. Giovannoni, M.R. Fisk, T.D. Mullins, H. Furnes, Genetic evidence for endolithic microbial life colonizing basaltic glass/seawater interfaces, Proc. ODP Sci. Results 148 (1996) 207–214.
[5] M.R. Fisk, S.J. Giovannoni, I. Thorseth, Alteration of oceanic volcanic glass textural evidence of microbial activity, Science 281 (1998) 978–980.
[6] T. Torsvik, H. Furnes, K. Muehlenbachs, I. Thorseth, O. Tumyr, Evidence for microbial activity at the glass-alteration interface in oceanic basalts, Earth Planet. Sci. Lett. 162 (1998) 165–176.
[7] H. Staudigel, A. Yayanos, R. Chastain, G. Davies, E.A.Th. Verdurmen, P. Schiffman, R. Bourcier, H. De-Baar, Biologically mediated dissolution of volcanic glass in seawater, Earth Planet. Sci. Lett. 164 (1998) 233–244.
[8] H. Furnes, H. Staudigel, Biological mediation in ocean crust alteration: how deep is the deep biosphere?, Earth Planet. Sci. Lett. 166 (1999) 97–103.
[9] H. Furnes, K. Muehlenbachs, O. Tumyr, T. Torsvik, I.H. Thorseth, Depth of active bio-alteration in the ocean crust

Costa Rica Rift (Hole 504B), Terra Nova 11 (1999) 228–233.
[10] J.L. Crovisier, J.H. Thomassin, T. Juteau, J.P. Eberhart, J.C. Touray, P. Baillif, Experimental seawater–basalt glass interaction at 50°C: study of early developed phases by electron microscopy and X-ray photoelectron spectrometry, Geochim. Cosmochim. Acta 47 (1983) 377–387.
[11] J.L. Crovisier, H. Atassi, V. Daux, J. Honnorez, J.C. Petit, J.P. Eberhart, A new insight into the nature of the leached layers formed on basaltic glasses in relation to the choice of constraints for long-term modeling, Mat. Res. Soc. Symp. Proc. 127 (1989) 41–48.
[12] G. Berger, J. Schott, M. Loubet, Fundamental processes controlling the first stage of alteration of a basalt glass by seawater: an experimental study between 200 and 320°C, Earth Planet. Sci. Lett. 84 (1987) 431–445.
[13] G. Berger, C. Clarparols, C. Guy, V. Daux, Dissolution rate of a basalt glass in silica-rich solutions: implications for long-term alteration, Geochim. Cosmochim. Acta 58 (1994) 4875–4886.
[14] C. Guy, J. Schott, Multisite surface reaction versus transport control during the hydrolysis of a complex oxide, Chem. Geol. 78 (1989) 181–204.
[15] J.C. Alt, C. Laverne, D. Vanko, P. Tartarotti, D.A.H. Teagle, W. Bach, E. Zuleger, J. Erzinger, J. Honnorez, P.A. Pezard, K. Becker, M.H. Salisbury, R.H. Wilkens, Hydrothermal alteration of a section of upper oceanic crust in the eastern equatorial Pacific: a synthesis of results from Site 504 (DSDP legs 69, 70 and 83, and ODP legs 111, 137, 140 and 148, Proc. ODP Sci. Results 148 (1996) 417–434.
[16] G.D. Guthrie, D.R. Veblen, Interpreting one-dimensional high-resolution transmission electron micrographs of sheet silicates by computer simulation, Am. Mineral. 75 (1990) 276–288.
[17] W.T. Jiang, D.R. Peacor, R.J. Merriman, B. Roberts, Transmission and analytical electron microscopic study of mixed-layer illite/smectite formed as an apparent replacement product of diagenetic illite, Clays Clay Miner. 38 (1990) 449–468.
[18] D.R. Peacor, Analytical electron microscopy: X-ray analysis, in: P.R. Buseck (Ed.), Minerals and Reactions at the Atomic Scale: Transmission Electron Microscopy, Reviews in Mineralogy 27, Min. Soc. Am., Chelsea, MI, 1992, pp. 113–140.
[19] J. Honnorez, La Palagonitisation, Birkhauser, Basel, 1967.
[20] J. Honnorez, The aging of the oceanic crust at low temperature, in: C. Emiliani (Ed.), The Sea, vol. 7, Wiley, New York, 1981, pp. 525–587.
[21] H. Staudigel, S.R. Hart, Alteration of basaltic glass: mechanisms and significance for the oceanic crust–seawater budget, Geochim. Cosmochim. Acta 47 (1983) 337–350.
[22] J.C. Petit, G. Della Mea, J.C. Dran, M.C. Magonthier, P.A. Mando, A. Paccagnella, Hydrated-layer formation during dissolution of complex silicate glasses and minerals, Geochim. Cosmochim. Acta 54 (1990) 1941–1955.
[23] J.C. Alt, Very low grade hydrothermal metamorphism of basic igneous rocks, in: M. Frey, D. Robinson (Ed.), Very Low Grade Metamorphism, Blackwell Scientific, London, 1999, pp. 169–201.
[24] W. Zhou, D.R. Peacor, J.C. Alt, R. Van der Voo, L.S. Kao, TEM study of the alteration of glass in MORB by inorganic processes, Chem. Geol. (1999), in press.
[25] O. Grauby, S. Petit, A. Decarraeu, A. Baronnet, The beidellite-saponite series: an experimental approach, Eur. J. Mineral. 5 (1993) 623–635.
[26] I.H. Thorseth, H. Furnes, O. Tumyr, A textural and chemical study of Icelandic palagonite of varied composition and its bearing on the mechanism of the glass-palagonite transformation, Geochim. Cosmochim. Acta 55 (1991) 731–749.
[27] J.L. Crovisier, J. Honnorez, J.P. Eberhart, Dissolution of basalt glass in seawater: mechanism and rate, Geochim. Cosmochim. Acta 51 (1987) 2977–2990.
[28] J.L. Crovisier, J. Honnorez, B. Fritz, J.C. Petit, Dissolution of subglacial volcanic glasses from Iceland: laboratory study and modeling, Appl. Geochem. 1 (1992) 55–81.
[29] Z. Zhou, W.S. Fyfe, Palagonitization of basaltic glass from DSDP Site 335, Leg 37: textures, chemical composition and mechanism of formation, Am. Mineral. 74 (1989) 1045–1053.
[30] G. Leturcq, G. Berger, T. Advocat, E. Vernaz, Initial and long term dissolution rates of aluminosilicate glasses enriched with Ti, Zr, and Nd, Chem. Geol. 160 (1999) 39–62.
[31] P.J.R. Uwins, R.I. Webb, A.P. Taylor, Novel nano-organisms from Australian sandstones, Am. Mineral. 83 (1998) 1541–1550.
[32] W.E. Seyfried, Experimental and theoretical constraints on hydrothermal alteration processes at Mid-ocean ridges, Ann. Rev. Earth Planet. Sci. 15 (1987) 317–335.
[33] H.I. Teng, D.E. Grandstaff, Dissolution of basaltic glass: effects of pH and organic ligands, Mat. Res. Soc. Symp. Proc. 412 (1996) 249–256.
[34] M.J. Eick, P.R. Grossl, D.C. Golden, D.L. Sparks, D.W. Ming, Dissolution kinetics of a lunar glass simulant at 25°C: the effect of pH and organic acids, Geochim. Cosmochim. Acta 60 (1996) 157–170.
[35] B.E. Kalinowski, L.J. Liermann, S.L. Brantley, A. Barnes, C.G. Pantano, X-ray photoelectron evidence for bacteria-enhanced dissolution of hornblende, Geochim. Cosmochim. Acta 64 (2000) 1331–1343.
[36] K.O. Konhauser, M.M. Urrutia, Bacterial clay authigenesis: a common biogeochemical process, Chem. Geol. 161 (1999) 399–416.
[37] A.J. Andrews, W.A. Dollase, M.E. Fleet, A Mossbauer study of saponite occurring in Layer 2 basalts, DSDP Leg 69, Initial Rep. DSDP 69 (1983) 585–588.
[38] A.C.D. Newman, G. Brown, The chemical constitution of clays, in: A.C. Newman (Ed.), Chemistry of Clays and

Clay Minerals, Min. Soc. Monogr. 6, Wiley, New York, 1987, pp. 1–128.
[39] I.S.E. Carmichael. M.S. Ghiorso, The effect of oxygen fugacity on the redox state of natural liquids and their crystallizing phases, in: J. Nicholls, K. Russell (Eds.), Modern Methods of Igneous Petrology: Understanding Magmatic Processes, Min. Soc. Am., Chelsea, 1990.
[40] J.C. Alt, T.F. Anderson, L. Bonnell, The geochemistry of sulfur in a 1.3 km section of hydrothermally altered oceanic crust, DSDP Hole 504B, Geochim. Cosmochim. Acta 53 (1989) 1011–1023.
[41] A.J. Andrews, On the effect of low-temperature seawater-basalt interaction on the distribution of sulfur in oceanic crust, layer 2, Earth Planet. Sci. Lett. 46 (1979) 68–80.
[42] J.C. Alt, W.C. Shanks, Sulfur in serpentinized oceanic peridotites: serpentinization processes and microbial sulfate reduction, J. Geophys. Res. 103 (1998) 9917–9929.